chemistry proceedings

MDPI

Proceeding Paper

Pyrene-4,5,9,10-Tetrachalcogenone Derivatives: A Computational Study of Their Potential Use as Materials for Batteries †

M. Pilar Vázquez-Tato [1], Francisco Meijide [2], Francisco Fraga [3], José Vázquez Tato [2] and Julio A. Seijas [1,*]

[1] Departamento de Química Orgánica, Facultade de Ciencias, Universidade de Santiago de Compostela, Campus Terra, 27080 Lugo, Spain; pilar.vazquez.tato@usc.es
[2] Departamento de Química Física, Facultade de Ciencias, Universidade de Santiago de Compostela, Campus Terra, 27080 Lugo, Spain; francisco.meijide@usc.es (F.M.); jose.vazquez@usc.es (J.V.T.)
[3] Departamento de Física Aplicada, Facultade de Ciencias, Universidade de Santiago de Compostela, Campus Terra, 27080 Lugo, Spain; francisco.fraga@usc.es
* Correspondence: julioa.seijas@usc.es
† Presented at the 26th International Electronic Conference on Synthetic Organic Chemistry, 15–30 November 2022; Available online: https://ecsoc-26.sciforum.net/.

Abstract: Polycyclic aromatic hydrocarbons are versatile building blocks for conjugated materials and can be applied in molecular electronics. Pyrenes are known as the best organic chromophores, and pyrene itself is known as an electron donor. Likewise quinones are promising electrode materials for lithium-ion batteries. The calculations were performed for: pyrene-4,5,9,10-tetrathione, pyrene-4,5,9,10-tetraselenone and pyrene-4,5,9,10-tetratellurone and comparing the results with those of pyrene-4,5,9,10-tetraone. The results obtained indicate that the sulfur derivative is a suitable candidate to carry out experimental studies, since although those of selenium and tellurium compounds also present better prospects than 4,5,9,10-tetraoxopyrene, they require the improvement of available synthetic techniques or even the discovery of new ones.

Keywords: pyrene-4,5,9,10-tetrachalcogenones; battery; organic electrode; DFT; reduction potential; sulfur; selenium; tellurium; cathode

Citation: Vázquez-Tato, P.; Meijide, F.; Fraga, F.; Tato, J.V.; Seijas, J.A. Pyrene-4,5,9,10-Tetrachalcogenone Derivatives: A Computational Study **of** Their Potential Use as Materials for Batteries. *Chem. Proc.* 2022, *4*, x. https://doi.org/10.3390/xxxxx

Academic Editor(s):

Published: 15 November 2022

Publisher's Note: MDPI stays neutral with regard to jurisdictional claims in published maps and institutional affiliations.

1. Introduction

Powered by the rising demand for large-scale electrochemical energy storage devices such as smart grids and electric vehicles, low-cost batteries with high energy density have become a major interest among sustainable energy research directions [1]. Within this target, organic electrode materials become rather promising candidates for lithium-ion batteries, since organic constituents usually have the advantages of higher recyclability and easier synthesis against inorganic compounds [2]. The lithium storage mechanism of organic carbonyl compounds relies on the redox reactions of the oxygen atom on the carbonyl group, which is able to undergo a reversible one-electron reduction to generate a radical anion combining with lithium ions [3]. Among other candidates, quinone derivatives have been studied experimentally as promising organic electrode materials, given that the reversible redox reactions occur between Li atoms and the carbonyl group. During discharging, the oxygen atom on each carbonyl group obtains an electron along with a lithium ion to form a lithium enol salt. While charging, lithium ions are released with electrons from the enol salts returning to the carbonyl groups. The reversible insertion and extraction of the lithium ions are achieved through the conversion between the carbonyl and enol structures. The main merits of the quinone compound cathode materials are great theoretical capacity (902 mA h g^{-1}) and high redox potential (3.0 V vs. Li/Li^+) [3], in particular pyrene-4,5,9,10-tetraketone (**1**, PTO) presents 409 mA h g^{-1} [4] and has been

studied in depth both experimentally and theoretical calculations [5]. This communication presents the theoretical study of reduction potential for chalcogen analogs of PTO, namely pyrene-4,5,9,10-tetrathione (**2**, PTS), pyrene-4,5,9,10-tetraselenone (**3**, PTSe) and pyrene-4,5,9,10-tetratellurone (**4**, PTTe) and comparing the results with those of pyrene-4,5,9,10-tetraone (Figure 1).

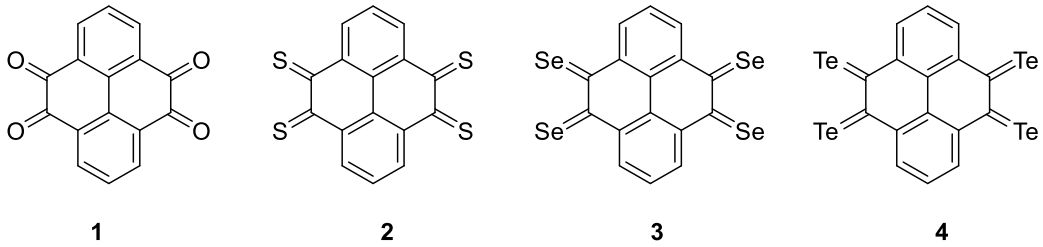

Figure 1. Pyrene-4,5,9,10-tetraketone (**1**, PTO), pyrene-4,5,9,10-tetrathione (**2**, PTS), pyrene-4,5,9,10-tetraselenone (**3**, PTSe) and pyrene-4,5,9,10-tetratellurone (**4**, PTTe).

2. Results and Discussion

Density functional theory (DFT) calculations were performed with the Gaussian 16 program package [6], at B3LYP/LANL2DZ level. For the solution calculations dimethyl sulfoxide (DMSO) was chosen (using a polarizable continuum model), due to its low toxicity and because it is a non-hazardous solvent that can solubilize a vast variety of organic compounds [7]. The vibrational frequency analysis was performed at the same level of theory and the obtained positive frequencies confirmed that the optimized geometries were found at the real minima on the potential energy surfaces.

Electron transfer during an electrochemical process leads to the reduction/oxidation of the compound. The redox ability of the compound can be quantitatively described by the redox potential. Consequently the performance of organic electrical devices is highly dependent on the oxidation potential (E_{OX}) and the reduction potential (E_{RED}) of the used materials. These potentials for the materials govern their capability to capture (or inject) holes and electrons, respectively, in the devices.

The thermodynamic cycle for the Gibbs free energy of the oxidation and reduction reaction of the molecule (A) is displayed in Scheme 2 [8].

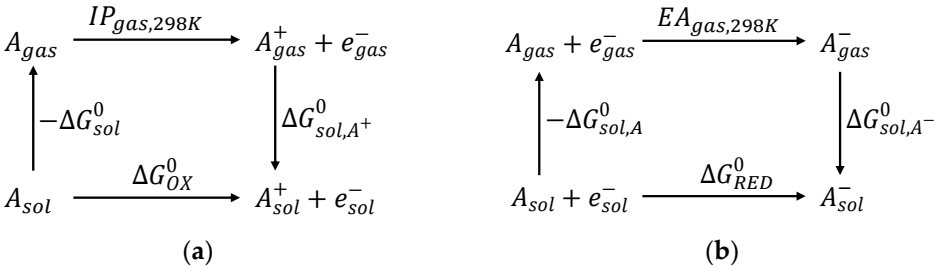

Scheme 2. Thermodynamic cycle for the Gibbs free energy of the (**a**) oxidation and (**b**) reduction reactions of a molecule.

The ΔG_{sol} is evaluated as the electronic energy difference of the molecule in the gas phase and the solvated one using the equilibrium geometry obtained in vacuum.

To estimate the charge transfer properties Marcus theory was used, according to this the reorganization energy (λ) has both intra- and intermolecular contributions. The former reflects the deformation of molecular geometry in order to accommodate charge transfer; and the latter reflects the electronic polarization of the surrounding molecules, being much smaller than the intramolecular one and is usually neglected. The intramolecular reorganization energy can be evaluated either from the adiabatic potential-energy

surfaces or from normal-mode analysis [9]. In this method, the hole and electron reorganization energies ($\lambda_{h/e}$) are defined by the following equation:

$$\lambda_{h/e} = \lambda^1 + \lambda^2$$

$$\lambda^1 = E_N(Q_{h/e}) - E_N(Q_N)$$

$$\lambda^2 = E_{h/e}(Q_N) - E_{h/e}(Q_{h/e})$$

where, $E_N(Q_N)$ and $E_{h/e}(Q_{h/e})$ are the ground-state energies of the optimized neutral and ionic states, respectively, $E_N(Q_{h/e})$ is the energy of the charged molecules at the optimal geometry of the neutral molecules, and $E_{h/e}(Q_N)$ is the energy of the neutral molecules at the optimal ionic geometry.

The adiabatic ionization potential $IP_{(a)}$ and adiabatic electron affinity $EA_{(a)}$ are two important parameters to evaluate the oxidation and reduction ability of charged organic molecules. Large $EA_{(a)}$ is beneficial for stabilizing the organic radical anions and decreases the electron injection energy barrier and, hence, it is helpful for electron transport [10]. Thus, the corresponding adiabatic IPs and EAs were obtained with following equations:

$$IP_{(a)} = E_h(Q_h) - E_N(Q_N)$$

$$EA_{(a)} = E_N(Q_N) - E_e(Q_e)$$

In evaluating electron rearrangement energy, the two alternatives are that either the transfer occurs with the motion of one electron, or it occurs simultaneously with several electrons at the same time [11]. In Figure 2 it is described the adiabatic potential energy surface method, which is used for calculating the reorganization energy, for dianion for both different cases: through the monoanion with transfer of one electron in two stages and when two electrons are transferred in a single process.

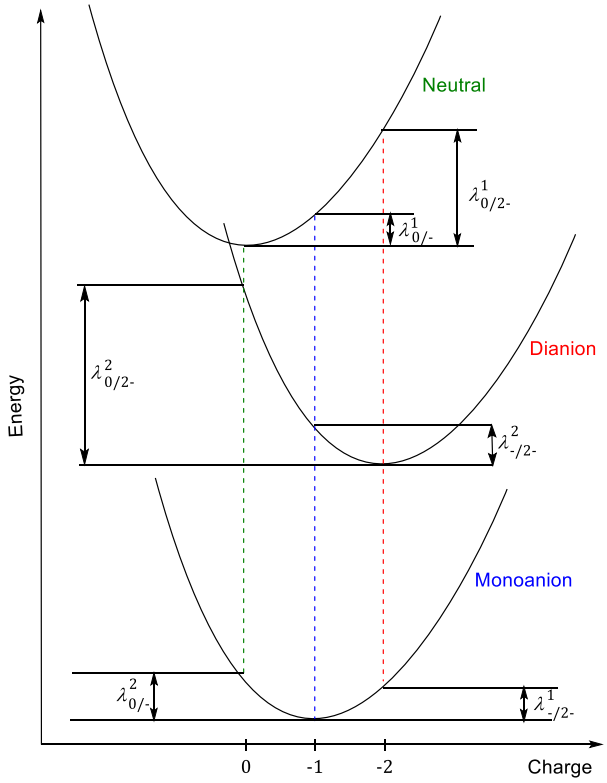

Figure 2. Schematic plot of reorganization energy for electron transfer for compounds PTO, PTS. PTSe and PTTe.

The redox potentials $[Z]^{0/-}$, $[Z]^{0/2-}$, $[Z]^{0/3-}$, $[Z]^{0/4-}$ of the different species resulting in the corresponding mono, di, tri and tetraanion (Scheme 1), were calculated as mentioned above, together with the corresponding electron reorganization energies (λ) to check the feasibility of the reduction process. Lower λ values are related to higher charge carrier mobility (Table 1).

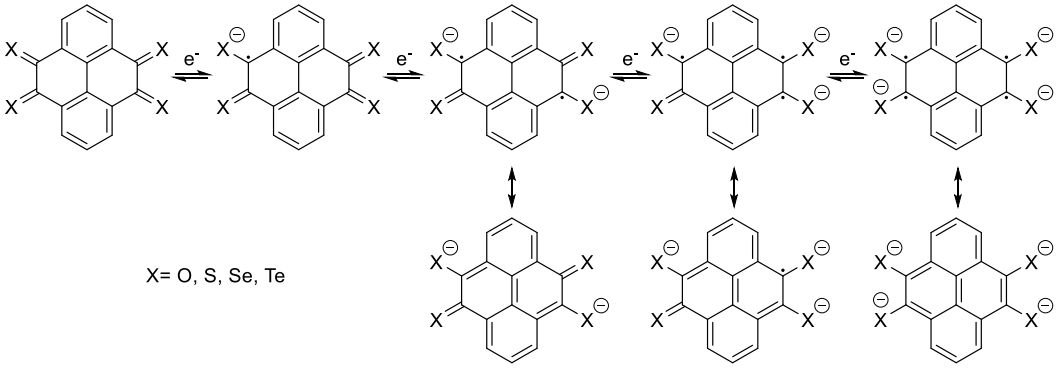

Scheme 1. Electron transfer in redox processes $[Z]^{0/-}$, $[Z]^{0/2-}$, $[Z]^{0/3-}$, $[Z]^{0/4-}$, and resonance structures of corresponding anions.

Table 1. Reduction potentials and electron reorganization energies for redox processes $[Z]^{0/-}$, $[Z]^{0/2-}$, $[Z]^{0/3-}$, $[Z]^{0/4-}$(b3lyp/lanl2dz).

Compound	PTO	PTS	PTSe	PTTe
$[Z]^{0/-}$	−4.35	−4.18	−4.17	−6.50
$[Z]^{0/2-}$	−7.55	−9.42	−7.77	−9.69
$[Z]^{0/3-}$	−10.61	−12.91	−11.88	−13.49
$[Z]^{0/4-}$	−12.58	−16.11	−14.96	−16.46
$\lambda_{0/-}$	0.14	2.22	0.87	0.58
$\lambda_{0/2-}$	0.99	3.51	3.13	2.12
$\lambda_{0/3-}$	1.80	4.58	5.39	4.32
$\lambda_{0/4-}$	2.92	8.17	8.70	7.04

The results for $[Z]^{0/-}$ calculation are similar, with lower potentials for PTS and PTSe, only in the case of tellurium the potential is clearly more negative than the one of PTS. For reduction to $[Z]^{0/2-}$ species, compound PTS resulted in −9.42 V, that is around −2 V difference with oxygen and selenium compounds and similar to the value of the compound with tellurium atoms. The same trend is found in the potentials $[Z]^{0/3-}$, $[Z]^{0/4-}$.Generally, lower λ values are related to higher charge carrier mobility and in the present study those of PTS, PTSe and PTTe are greater than that of PTO.

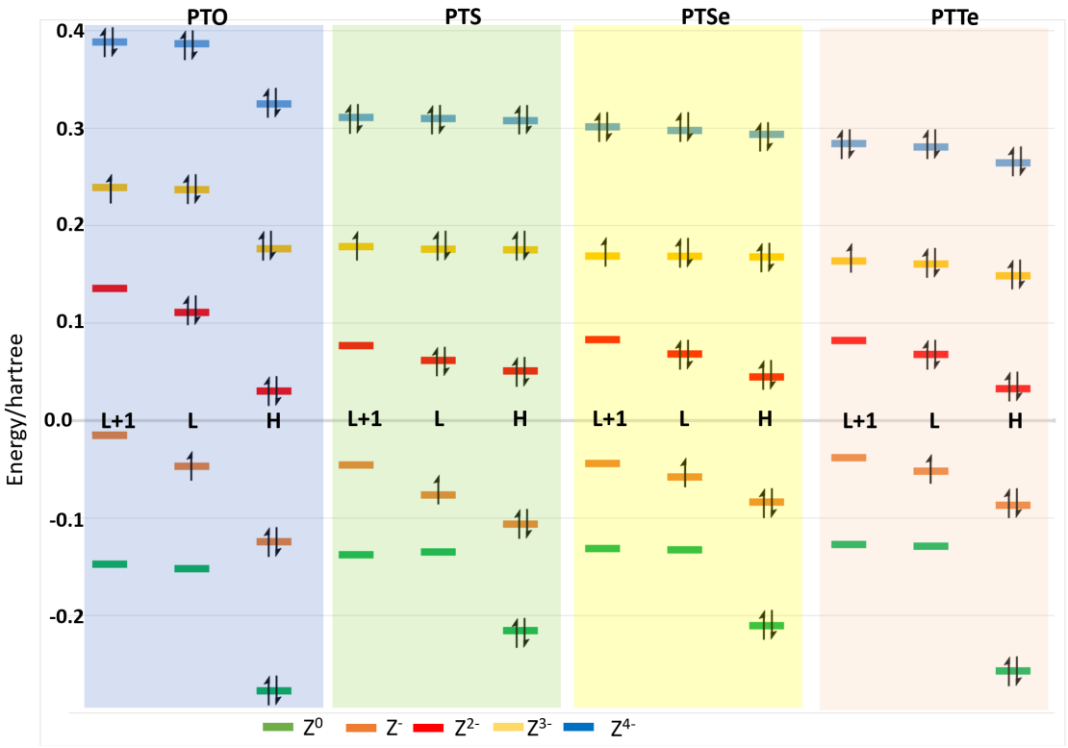

Figure 2. Schematic plot of the orbitals energy HOMO (H), LUMO (L) and LUMO + 1 (L + 1) for neutral compounds PTO, PTS, PTSe, and PTTe, and charged species −1, −2, −3 and −4. In each orbital the occupancy is showed.

Figure 2 shows the energy of the orbitals in outer shell for PTO, PTS, PTSe and PTTe, indicating for each compound the HOMO, LUMO and LUMO + 1 of the neutral species, where gained electrons throughout the reduction process are located. The energy difference between the orbitals of each charged species is similar for PTS, PTSe and PTTe, being the difference between HOMO and LUMO higher for the PTO than in the other compounds.

The values for PTS indicated in Table 2 show, as mentioned above, a value for $\lambda_{(0/-)}$ that is high when compared to those obtained for the other compounds. Highlight that there is at least an additional possible geometry (Figure 3b), not as flat as the previous one (Figure 3a), with the sulfur atoms out of the plane of the rings, which also meets the requirement of lacking vibrations with a negative value and therefore corresponds to a minimum on the potential energy surface. The neutral non planar conformation of PTS is 2.32 Kcal/mol more stable in vacuum and 3.70 Kcal/mol in DMSO as solvent.

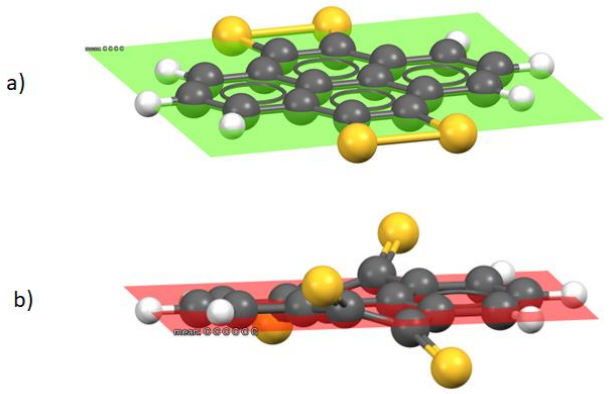

Figure 3. Conformers of compound PTS, (**a**) sulfur atoms coplanar to the ring, (**b**) sulfur atoms out-of-plane of the carbon skeleton.

This out-of-plane structure for PTS (Figure 3b) was used to calculate the reduction potentials in order to obtain the corresponding anions ($[Z]^{0/-}$, $[Z]^{0/2-}$, $[Z]^{0/3-}$, $[Z]^{0/4-}$), as well as their electronic rearrangement energies (λ). The new values for the reduction potentials turned out to be less negative, and the rearrangement energies suffered a significant reduction as is collected in Table 2.

Table 2. Reduction potentials and electron reorganization energies for redox processes $[Z]^{0/-}$, $[Z]^{0/2-}$, $[Z]^{0/3-}$, $[Z]^{0/4-}$(b3lyp/lanl2dz) for PTS and its conformer with sulfur atoms out-of-plane of the carbon skeleton.

Compound	PTS	PTS Out-of-Plane
$[Z]^{0/-}$	−4.18	−4.59
$[Z]^{0/2-}$	−9.42	−8.54
$[Z]^{0/3-}$	−12.91	−12.61
$[Z]^{0/4-}$	−16.11	−15.91
$\lambda_{0/-}$	2.22	0.26
$\lambda_{0/2-}$	3.51	0.91
$\lambda_{0/3-}$	4.58	1.92
$\lambda_{0/4-}$	8.17	3.30

This new spatial arrangement for PTS also influences the energy of the orbitals involved in the transfer of electrons in LUMO + 1, LUMO and HOMO, that are indicated comparatively in Figure 4, noting that fundamentally affects those of the neutral molecule and the monoanion. Thus, for the neutral molecule the energy difference is clear for the three orbitals (LUMO + 1, LUMO and HOMO, 0.53 eV, 0.72 eV, and 0.52 eV) decreasing for the monoanion (LUMO + 1, LUMO and HOMO, 0.10 eV, 0.28 eV, and 0.28 eV). For the di-, tri- and tetra anion this difference declines almost completely, since with the gain of electrons the sulfur atoms are located in the plane of the pyrene rings.

Figure 4. Schematic plot of the HOMO, LUMO and LUMO + 1 orbital energies for the conformers of PTS with planar sulfur (p) and out-of-plane sulfur (oop) in the, −1, −2, −3 and −4 species.

3. Conclusions

The computational results obtained point out that the pyrene-4,5,9,10-tetrathione is a suitable candidate to carry out experimental studies to check its suitability as material for electrode in batteries, since although pyrene-4,5,9,10-tetraselenone and pyrene-4,5,9,10-tetratellurone also present better prospects than 4,5,9,10-tetraoxopyrene, they require the improvement of available synthetic techniques or even the discovery of new ones, meanwhile, plenty of methods for the thionation of carbonyl compounds are available in the literature [12].

Author Contributions:

Funding: This work was funded by the Ministerio de Ciencia y Tecnología, Spain (Project MAT201786109P).

Institutional Review Board Statement:

Informed Consent Statement:

Data Availability Statement:

Conflicts of Interest:

References

1. Miao, L.; Liu, L.; Shang, Z.; Li, Y.; Lu, Y.; Cheng, F.; Chen, J The structure–electrochemical property relationship of quinone electrodes for lithium-ion batteries. *Phys.Chem.Chem.Phys.* **2018**, *20*, 13478–13484. https://doi.org/10.1039/c8cp00597d.
2. Armand, M.; Tarascon, J.M. Building better batteries. *Nature* **2008**, *451*, 652–657. https://doi.org/10.1038/451652a.
3. Lyu, H.; Sun, X.G.; Dai, S. Organic Cathode Materials for Lithium-Ion Batteries: Past, Present, and Future. *Adv. Energy Sustainability Res.* **2021**, *2*, 2000044. https://doi.org/10.1002/aesr.202000044.
4. Zhu, Z.; Hong, M.; Guo, D.; Shi, J.; Tao, Z.; Chen, J. All-Solid-State Lithium Organic Battery with Composite Polymer Electrolyte and Pillar [5]quinone Cathode. *J. Am. Chem. Soc.* **2014**, *136*, 16461–16464. https://doi.org/10.1021/ja507852t
5. Zhang, M.; Zhang, Y.; Huang, W.; Zhang, Q. Recent Progress in Calix[n]quinone (n=4, 6) and Pillar [5]quinone Electrodes for Secondary Rechargeable Batteries. *Batter. Supercaps* **2020**, *3*, 476–487. https://doi.org/10.1002/batt.202000038
6. Yoo, G.; Pyo, S.; Gong, Y.J.; Cho, J.; Kim, H.; Kim, Y.S.; Yoo, J.J.C. Highly reliable quinone-based cathodes and cellulose nanofiber separators: Toward eco-friendly organic lithium batteries. *Cellulose* **2020**, *27*, 6707–6717. https://doi.org/10.1007/s10570-020-03266-8.
7. Shi, J.L.; Xiang, S.Q.; Su, D.:J.; He, R.X.; Zhao, L.B. Revealing practical specific capacity and carbonyl utilization of multi-carbonyl compounds for organic cathode materials. *Phys. Chem. Chem. Phys.* **2021**, *23*, 13159–13169. https://doi.org/10.1039/d1cp01645h.
8. Frisch, M.J.; Trucks, G.W.; Schlegel, H.B.; Scuseria, G.E.; Robb, M.A.; Cheeseman, J.R.; Scalmani, G.; Barone, V.; Petersson, G.A.; Nakatsuji, H.; et al. *Gaussian 16, Revision C.01*; Gaussian, Inc.: Wallingford, CT, USA, 2016.
9. Wang, M.; Dong, X.; Escobar, I.C.; Cheng, Y.-T. Lithium Ion Battery Electrodes Made Using Dimethyl Sulfoxide(DMSO) A Green Solvent. *ACS Sustain. Chem. Eng.* **2020**, *8*, 11046–11051. https://doi.org/10.1021/acssuschemeng.0c02884.
10. Wang, D.; Huang, S.-P.; Wang, C.; Yue, Y.; Zhang, Q.-S. Computational Prediction for Oxidation and Reduction Potentials of Organic Molecules Used in Organic Light-Emitting Diodes. *Org. Electron.* **2019**, *64*, 216–222. 10.1016/j.orgel.2018.10.038.
11. Shoaib, M.; Bibi, S.; Ullah, I.; Jamil, S.; Iqbal, J.; Alam, A.; Saeed, U.; Bai, F.Q. Theoretical Investigation of Perylene Diimide derivatives as Acceptors to Match with Benzodithiophene based Donors for Organic Photovoltaic Devices. Z. *Phys. Chem.* **2021**, *235*, 427–449. https://doi.org/10.1515/zpch-2019-1451.
12. Ji, L.-F.; Fan, J.-X.; Zhang, S.-F.; Ren, A.-M. Theoretical investigations into the charge transfer properties of thiophene α-substituted naphthodithiophene diimides: Excellent n-channel and ambipolar organic semiconductors. *Phys.Chem. Chem. Phys.* **2017**, *19*, 13978–13993. https://doi.org/10.1039/C7CP01114H.
13. Evans, D.H. One-Electron and Two-Electron Transfers in Electrochemistry and Homogeneous Solution Reactions. *Chem. Rev.* **2008**, *108*, 2113–2144. https://doi.org/10.1021/cr068066l.
14. Organic Chemistry Portal. Available online: https://www.organic-chemistry.org/synthesis/C2S/thioketones.shtm (accessed on 17 October 2022).